Solid State Nuclear Magnetic Resonance 100 (2019) 1–10

Contents lists available at ScienceDirect

Solid State Nuclear Magnetic Resonance

journal homepage: www.elsevier.com/locate/ssnmr

Sensitivity improvement in 5QMAS NMR experiments using FAM-N pulses

Nasima Kanwal [a], Henri Colaux [b,c], Daniel M. Dawson [a], Yusuke Nishiyama [b,d,e], Sharon E. Ashbrook [a,*]

[a] School of Chemistry, EaStCHEM and Centre of Magnetic Resonance, University of St Andrews, St Andrews, KY16 9ST, UK
[b] RIKEN-JEOL Collaboration Center, Tsurumi, Yokohama, Kanagawa, 230-0045, Japan
[c] Center for Surface Chemistry and Catalysis, KU Leuven, 3001, Heverlee, Belgium
[d] JEOL RESONANCE Inc., Musashino, Akishima, Tokyo, 196-8558, Japan
[e] NMR Science and Development Division, RIKEN SPring-8 Center, Tsurumi, Yokohama, Kanagawa, 230-0045, Japan

ARTICLE INFO

Keywords:
MQMAS
Five-quantum MAS
High-resolution NMR
Quadrupolar nuclei
Solid-state NMR spectroscopy

ABSTRACT

The multiple-quantum magic-angle spinning (MQMAS) experiment is a popular choice for obtaining high-resolution solid-state NMR spectra of quadrupolar nuclei with half-integer spin quantum number. However, its inherently poor sensitivity limits its application in more challenging systems. In particular, the use of higher-order multiple-quantum coherences, which have the potential to provide higher resolution in the isotropic spectrum, results in a further decrease in sensitivity. Here we extend our recent work, which introduced an automated, high-throughput approach to generate amplitude-modulated composite pulses (termed FAM-N) to improve the efficiency of the conversion of three-quantum coherences, and explore the use of similar pulses in five-quantum MAS experiments. We consider three different approaches, and are able to demonstrate that all three provide good enhancements over single pulse conversion in all but the most extreme cases, and work well at a range of spinning rates. We show that FAM-N pulses are robust to variation in the quadrupolar coupling and rf nutation rate, demonstrating their applicability in multisite systems and systems where direct experimental optimisation of complex composite pulses is not feasible. This work will ease the implementation of higher-order MQMAS experiments and enable their application to materials and systems that were previously deemed too difficult to study.

1. Introduction

Magic angle spinning (MAS) plays a vital role in NMR spectroscopy of solid materials, removing the anisotropic broadening that results from the orientation dependence of the interactions that affect the nuclear spins [1–3]. However, NMR spectra of nuclei with spin quantum number $I > 1/2$ remain broadened even under rapid sample rotation, as spinning around a single angle is not able to completely average the second-order quadrupolar broadening [2–4]. These quadrupolar nuclei, including ^{17}O, ^{23}Na, ^{27}Al, ^{25}Mg, ^{45}Sc and ^{71}Ga, are present in many materials of technological and industrial importance, and account for 75% of the magnetically-active nuclides in the Periodic Table. Therefore, the complete removal of quadrupolar broadening, and the acquisition of high-resolution spectra, is a constant challenge for solid-state NMR spectroscopy. Early solutions to this problem involved rotating the sample around more than one angle, simultaneously in the case of double rotation (DOR) [5], and sequentially for dynamic angle spinning (DAS) [6]. However, these technically challenging approaches have been largely superceded by the multiple-quantum (MQ) MAS experiment [4–7], introduced by Frydman and Harwood in 1995. This enables high-resolution spectra to be obtained using only conventional hardware, by correlating multiple-quantum coherences, usually triple-quantum (3Q), *i.e.*, $m_I = +3/2 \leftrightarrow m_I = -3/2$, with central-transition (CT), *i.e.*, $m_I = +1/2 \leftrightarrow m_I = -1/2$, coherences in a two-dimensional experiment. This approach has gained considerable popularity, and is widely used for the study of ceramics, microporous materials, energy materials, glasses and minerals [8,9].

The main drawback of MQMAS is the inherently poor sensitivity that results from filtration through multiple-quantum coherences [8–11]. More recently, Gan introduced the satellite-transition (ST) MAS experiment [12,13], which is conceptually similar to MQMAS, but correlates the purely single-quantum ST (*i.e.*, $m_I = \pm 1/2 \leftrightarrow m_I = \pm 3/2$) and CT coherences. Although this experiment offers a significant sensitivity advantage over MQMAS (usually a factor of 2–8), it is technically more

* Corresponding author.
E-mail address: sema@st-andrews.ac.uk (S.E. Ashbrook).

https://doi.org/10.1016/j.ssnmr.2019.03.002
Received 6 February 2019; Received in revised form 11 March 2019; Accepted 11 March 2019
Available online 15 March 2019

demanding to implement, requiring the spinning angle to be set very accurately (to within ~0.001°) and the spinning rate to be very stable (to within ±1 Hz) [13]. As a result, attention has continued to focus on improving the sensitivity of MQMAS experiments. The majority of these experiments involve triple-quantum coherences, and a number of approaches have been employed to improve the sensitivity of the (relatively inefficient) pulse that converts multiple-to single-quantum coherences [14–20]. Significant enhancements have been demonstrated using double frequency sweeps (DFS) [15], fast amplitude modulation (FAM-I and FAM-II) [14,16,17], soft pulse added mixing (SPAM) [14,18,19] and hyperbolic secant (HS) [20] pulses.

MQMAS experiments using higher-order multiple-quantum coherence are also possible [21]. As discussed by Wimperis and co-workers [22], such experiments can, in principle, offer greater resolution providing the linewidth in the isotropic dimension of the spectrum is dominated by homogeneous contributions. Although this resolution advantage has been exploited in the study of microporous materials [23–26], minerals [27,28] and inorganic solids [29–31], such experiments have not been widely applied, largely as a result of the significant loss in sensitivity that accompanies an increase in the order of the multiple-quantum coherences used. This can be seen in Fig. 1a, which compares ^{27}Al conventional, triple-quantum (3Q) and five-quantum (5Q) filtered MAS NMR spectra of Al(acac)$_3$. A significant decrease in intensity (by a factor of ~8) is observed upon filtration through 3Q coherences, and a further reduction (by a factor of ~5) is seen, when 5Q coherences are used. Fig. 1b shows how the theoretical relative efficiencies of ^{27}Al 3Q and 5Q filtration (simulated using optimised pulses with an rf nutation rate of $\nu_1 = 100$ kHz, an MAS rate of 12.5 kHz at an external field strength of 14.1 T) vary with the magnitude of the quadrupolar coupling constant, C_Q. The 5Q filtered signal drops more rapidly with an increase in C_Q, although both transfers exhibit poor efficiency as C_Q increases. Surprisingly, however, there has been considerably less effort focussed on improving the conversion efficiency in 5QMAS experiments. Work by Iuga et al. used DFS for the conversion of 5Q coherences in ^{27}Al NMR spectra of $9Al_2O_3.2B_2O_3$, although the exact enhancement factor achieved was not clear, and significant lineshape distortions were observed [32]. The sequential application of two FAM-I conversion pulses (aimed at performing 5Q → 3Q and 3Q → CT transfer) by Vosegaard et al. [33] for the same compound gave a sensitivity enhancement of ~2. Brauniger et al. [34] also investigated both single and sequential blocks of FAM-I and FAM-II pulses for 5Q → CT transfer, achieving similar efficiencies experimentally. Goldbourt et al. have investigated more generally the use of two FAM-II conversion pulses for 5QMAS experiments [35]. It should also be noted that Refs. [34,35] have both employed FAM pulses for the excitation of 5Q coherences. While these were shown to give enhancements over single pulse excitation (and, therefore, further sensitivity gains when considering the MQMAS sequence as a whole), these gains do tend to be lower than those obtained when the conversion pulse is considered. The large number of experimental and pulse sequence parameters that are involved when modulation of both excitation and conversion pulses is considered makes direct comparison difficult. However, Brauniger et al. [34] achieved an experimental signal enhancement of ~3 for Al(acac)$_3$ with modulation of both excitation and conversion pulses.

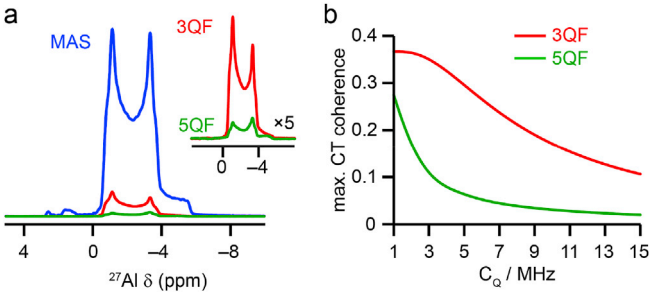

Fig. 1. (a) ^{27}Al (14.1 T, 12.5 kHz) conventional (blue), 3Q filtered (red) and 5Q filtered (green) MAS NMR spectra of Al(acac)$_3$, acquired with $\nu_1 \approx 100$ kHz. Spectra are the result of averaging 960 transients with a recycle interval of 3 s. (b) Maximum amount of ^{27}Al single-quantum CT coherence generated from filtration through 3Q (red) and 5Q (green) coherences as a function of C_Q. Simulated using $\nu_1 = 100$ kHz, $\nu_R = 12.5$ kHz, $\eta_Q = 0$ and $B_0 = 14.1$ T, with optimised pulses in all cases.

Although FAM-II pulses offer a relatively simple approach to signal enhancement for MQ conversion, experimental optimisation can be challenging and time consuming, particularly when the sensitivity is low (*i.e.*, where such pulses are vital), and as the number of pulses used increases. This either limits the number of pulses that can be used practically, or requires the imposition of some restriction where the duration of earlier pulses in the sequence are fixed, or do not vary upon addition of subsequent pulses. Recently, we demonstrated an efficient automated optimisation procedure for 3QMAS experiments that was able to determine the optimum number and duration of the components of a FAM pulse to be determined using numerical simulation, resulting in a "FAM-N″ pulse (a pulse with N sequential but oppositely-phased components) [36,37]. This approach places no constraint on the relative lengths of individual pulses (unlike previous work [38]), and the preceding pulse in the sequence is reoptimised automatically when the subsequent pulse is added, enabling higher efficiencies to be generated. FAM-N pulses can be generated easily, produce good signal enhancements for spin I = 3/2, 5/2, 7/2 and 9/2 nuclei, and can be typically be used without experimental reoptimisation [36,37]. The pulses have also been shown to be robust to reasonable variations in the experimental parameters, enabling them to be applied without prior knowledge of the system, and to materials where sites with different NMR parameters are present.

In this work, we extend our automated FAM-N approach to 5QMAS experiments, and specifically to the conversion of 5Q coherences. Using a model system, we consider three different approaches for generating FAM-N pulses for the conversion of 5Q coherences, and compare how they perform (relative to each other and to the use of a single pulse) both in simulation and experimentally. We also explore how the relative efficiencies of these pulses vary with changes in the MAS rate and the magnitude of the quadrupolar coupling constant. Finally, we show how these approaches can be used to improve sensitivity in more challenging systems, including ^{17}O (I = 5/2) NMR spectroscopy of silicate minerals (where sensitivity is often a major challenge, even when isotopic enrichment is possible) and ^{45}Sc (I = 7/2) NMR spectroscopy of a system with large quadrupolar couplings.

2. Experimental details

FAM-N pulses were generated using a high-throughput optimisation procedure that calls the density matrix simulation program SIMPSON [39] from an in-house MATLAB script, as outlined in Ref. [36], for user specified values of the external magnetic field strength (B_0), the MAS rate (ν_R), the inherent radiofrequency nutation rate (ν_1) and the quadrupolar parameters ($C_Q = eQV_{zz}/h$ and $\eta_Q = (V_{xx} - V_{yy})/V_{zz}$). Typically, 320 × 20 crystallites were used. The composite pulses produced can be written directly into pulse programs for either MQ filtered or two-dimensional MQMAS experiments in place of the conventional conversion pulse.

Three different approaches were considered for the conversion of 5Q coherences into CT coherences. The FAM-N pulses generated are used in place of the single conversion pulse shown in the sequence in Fig. 2.

(i) *Direct method:* a FAM-N pulse is generated by optimizing the amount of single-quantum CT coherences (*i.e.*, density matrix element {3, 4} for I = 5/2) produced directly from an initial unit amount of 5Q coherence of the same sign (*i.e.*, density matrix element {1, 6}). An example of the optimisation of this type of pulse is shown in Fig. 3a.

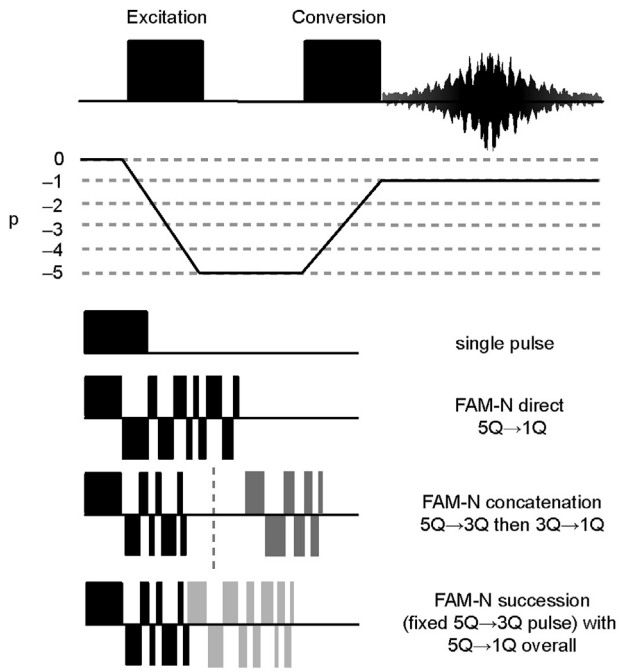

Fig. 2. Pulse sequence and coherence transfer pathway diagram for a 5Q filtered NMR experiment. The conversion of 5Q to CT coherences can be achieved using a single pulse or one of three different types of FAM-N pulse.

(ii) *Concatenation method:* two FAM-N pulses are optimised completely independently. The first optimizes the efficiency of the conversion of a unit amount of 5Q coherence (*i.e.*, {1, 6}) to (symmetrical) 3Q coherence of the same sign (*i.e.*, element {2, 5}). The second maximizes the creation of CT coherences from an initial unit amount of 3Q coherence, as described in earlier work [36,37]. These two pulses are then simply concatenated to produce the composite FAM-N pulse used experimentally. An example of this two-step optimisation is shown in Fig. 3b.

(iii) *Succession method:* the FAM-N pulse optimised for the conversion of 5Q to 3Q (described above) is used as an initial pulse train applied within a full optimisation of a final FAM-N pulse generated by maximizing the creation of CT coherences from an initial unit amount of 5Q coherence. Therefore, the initial train (with the exception of the last pulse) is not reoptimised in the second step, but used as is. An example of the optimisation of this type of pulse is shown in Fig. 3c.

As described in more detail in Refs. [36,37], in all optimizations the amount of desired coherence generated (be it 3Q or CT) is monitored as the duration of the rf pulse is varied. The duration of the first pulse is fixed at that producing the maximum coherence transfer, and a second pulse is applied with inverted phase. The duration of this pulse is incrementally varied (typically in steps of 2°, although this can be chosen by the user). The duration of the first pulse is then increased and the variation of the second pulse is repeated. This procedure is carried out repeatedly until additional increments decrease the maximum coherence transfer. At this point the next pulse is added, again with opposite phase and the whole procedure (varying the duration of final and penultimate pulses) is repeated. The optimisation is terminated when adding a new pulse does not increase the conversion efficiency.

Experimental NMR spectra were acquired using 14.1 T or 20.0 T Bruker Avance III spectrometers. Samples were packed in 4 mm, 3.2 mm, 1.9 mm or 1.3 mm rotors, and rotated at MAS rates of 12.5 kHz (4 mm), 20 kHz (3.2 mm), 40 kHz (1.9 mm) or 60 kHz (1.3 mm). Details of the rf nutation rates, MAS rates and FAM-N pulses used can be found in the relevant figure captions and in the Supporting Information. Chemical shifts are referenced to 1.1 M $Al(NO_3)_3$ (aq), H_2O and 0.06 M $Sc(NO_3)_3$ (aq) for ^{27}Al, ^{17}O and ^{45}Sc, respectively, determined using secondary solid references of $Al(acac)_3$ at $\delta_{iso} = 0$ ppm, MgO at $\delta_{iso} = 26$ ppm and $LaScO_3$ at $\delta_{iso} = 162$ ppm. MQ filtration experiments were performed with the selection of a $p = -5 \rightarrow -1$ coherence transfer pathway using an experimentally optimised single pulse for 5Q excitation, and either a single pulse or a FAM-N pulse for conversion. As shown in Refs. [36,37], experimental optimisation of the rf field strength (for fixed FAM-N pulse durations) can lead to small improvements in signal intensity, but in this work pulses were used directly in the experiment without any reoptimisation. However, the single pulses used for 5Q conversion were optimised directly in the experiment (leading in some cases to small differences in the sensitivity gains observed experimentally and in simulation).

3. Results and discussion

Fig. 4 plots the maximum ^{27}Al CT coherence generated (in simulation) from unit 5Q coherences using either a single pulse or one of the three different FAM-N pulses, as a function of C_Q. The simulations were carried out for $B_0 = 14.1$ T and an rf nutation rate of $\nu_1 = 80$ kHz for three different MAS rates. Note that the efficiency shown is that obtained with the optimum pulse for each C_Q (*i.e.*, the exact pulse employed varies for each data point). At the lowest MAS rate, all three FAM-N methods give increased conversion efficiency over the single pulse for all values of C_Q. The efficiency of each pulse decreases with increasing C_Q, although the rate of this decrease initially is greatest for a single pulse (in agreement with previous literature [21]), giving larger FAM-N enhancements (although lower overall signal) at moderate C_Q values, but a slight decrease in the enhancement at higher C_Q values. As the MAS rate increases the absolute efficiency of the FAM-N pulses decreases slightly, particularly at higher C_Q, although significant enhancements over single pulse conversion are still observed. This is similar to the behaviour observed previously for FAM-N pulses in 3QMAS experiments [37]. The three types of FAM-N approaches used generally have similar efficiencies, although for lower C_Q values the concatenation approach has slightly poorer efficiency, particularly at higher MAS rates.

Fig. 5 shows a similar plot of the maximum ^{27}Al CT coherence (generated from unit 5Q coherences using FAM-N or a single pulse), now as a function of the strength of the rf field, ν_1. Simulations were performed with for $B_0 = 14.1$ T, $C_Q = 3$ MHz at three different MAS rates, and the value plotted is that obtained for pulses optimised independently for each value of ν_1. Again, significant sensitivity gains over a single pulse are predicted for all three FAM-N methods at all MAS rates. However, the efficiency of the single pulse conversion rises more quickly with an increase in ν_1, resulting in a lower signal enhancement (despite an increase in absolute signal intensity in many cases) at higher rf nutation rates. At the lower MAS rates, the efficiency of the three FAM-N methods increases with the rf field strength (at least for lower ν_1), whereas as the highest MAS rate (60 kHz) the FAM-N efficiencies do not vary significantly as the rf nutation rate changes. For most conditions, although similar efficiencies are observed for all FAM-N methods, the efficiency of the concatenation approach is usually predicted to be slightly poorer. The difference in efficiency between the succession and concatenation approaches (which utilise the same initial pulse train) could result from either (i) the non-uniform conversion of multiple-quantum coherences in a powder distribution of crystallites or (ii) the presence of additional (i.e., non 3Q) coherences following the initial pulse train, neither of which are considered (or, perhaps more importantly, exploited) in the concatenation approach.

The relative experimental efficiencies of the three FAM-N approaches are compared in Fig. 6, which shows ^{27}Al (14.1 T) 5Q filtered MAS NMR spectra of $Al(acac)_3$, acquired at varying MAS rates and two different rf nutation rates (using an experimentally optimised excitation pulse in each case). Spectra acquired using a single pulse for 5Q conversion are also shown. This material has a single Al site with ^{27}Al $C_Q = 3$ MHz

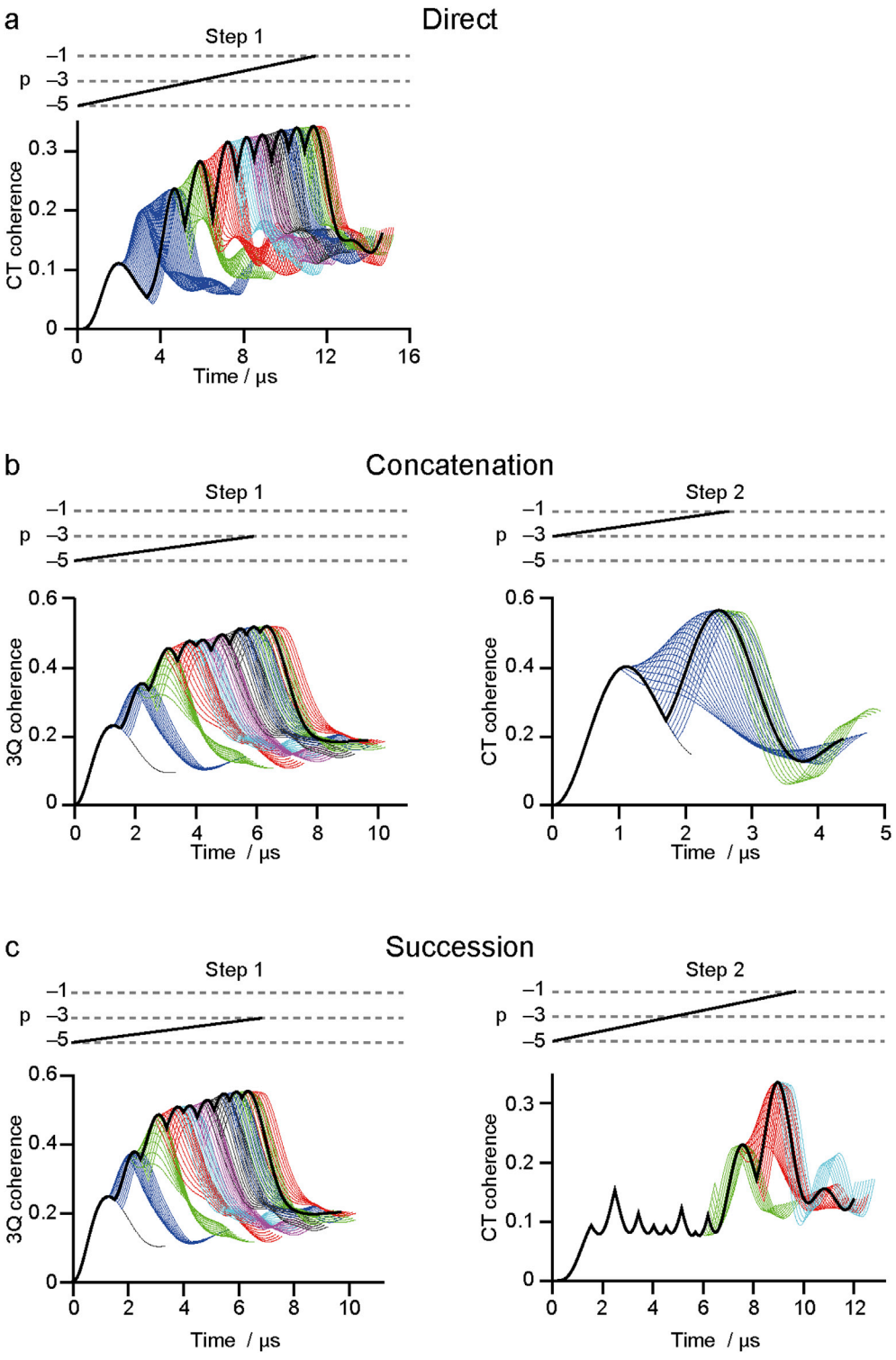

Fig. 3. Schematics showing the results of FAM-N optimizations (and the coherence transfers taking place) for the conversion of ^{27}Al 5Q to CT coherences (using $\nu_1 = 100$ kHz, $\nu_R = 12.5$ kHz, $C_Q = 3$ MHz, $\eta_Q = 0.15$ and $B_0 = 14.1$ T) for the (a) direct, (b) concatenation and (c) succession methods. A full description of the optimisation process in each case can be found in the text. The colours represent optimizations of the Nth pulse in the sequence. The black lines show the evolution of the desired (3Q or CT) coherence for the final (optimised) FAM-N pulse.

($\nu_Q^{PAS} = 3C_Q/4I(2I-1) = 225$ kHz) and $\eta_Q = 0.15$ [40]. At the lowest MAS rate, maximum signal enhancements, I/I_0, of ~1.7 ($\nu_1 = 100$ kHz) and ~2.1 ($\nu_1 = 60$ kHz) are observed, where I_0 is the signal intensity obtained using a single pulse for conversion and I is the signal intensity obtained when a FAM-N pulse is used. In both cases, there is relatively little difference in efficiency between the three FAM-N approaches, with the direct method slightly more efficient at higher rf nutation rate. All spectra show a distortion of the characteristic second-order quadrupolar lineshape, (as expected for MQMAS experiments, where the efficiency of excitation depends on the value of ν_Q, *i.e.*, upon crystallite orientation), but the distortions are similar for each conversion method, and generally similar to that seen for single pulse conversion. Less distortion is seen as the rf nutation rate increases, as expected. At 40 kHz MAS, the relative enhancement of the FAM-N pulses (over a single pulse) is better at an rf nutation rate of 60 kHz ($I/I_0 \approx 3.2$) than at 100 kHz ($I/I_0 \approx 2.2$), perhaps reflecting the relatively poor efficiency of the single pulse conversion as the rf drops. At the lower rf nutation rate the succession method has marginally better sensitivity, while at the higher rate the direct method has the higher efficiency. The signal-to-noise obtained at the highest MAS rate is poorer (owing to the very small sample volume present), but it is

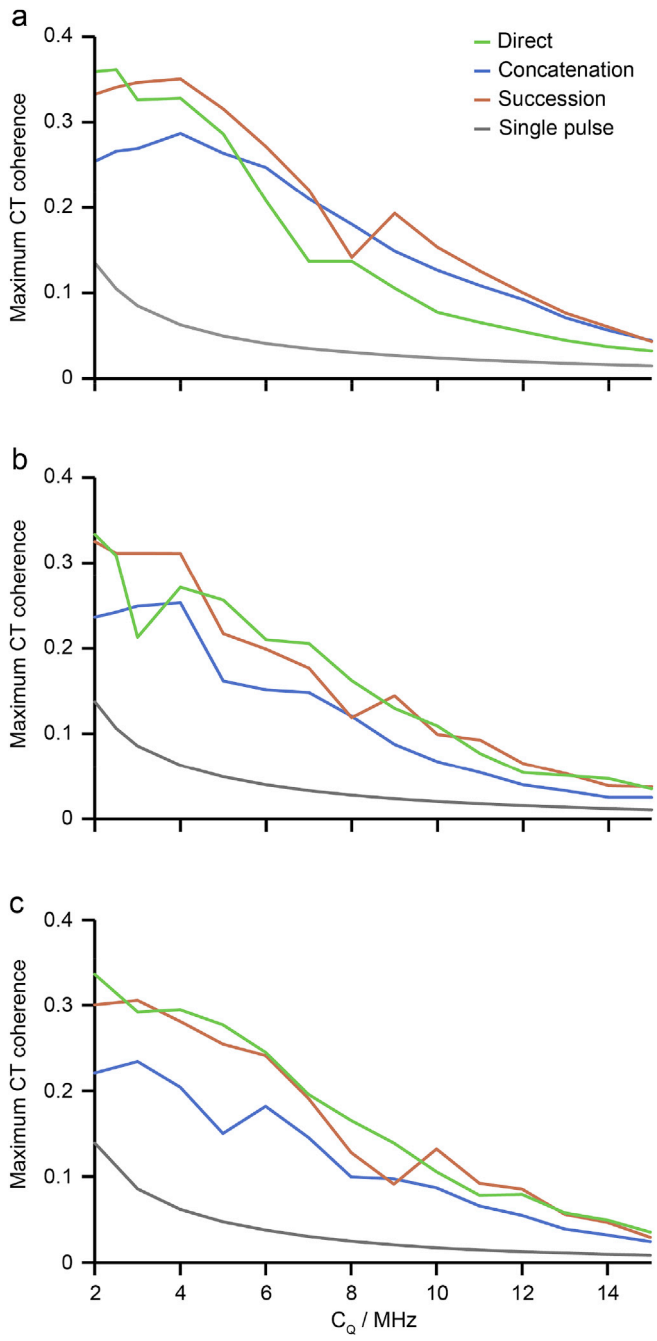

Fig. 4. Plots of the maximum CT coherence obtained from unit 5Q coherence using an optimised single pulse (grey), or FAM-N pulses generated using the direct (green), concatenation (blue) and succession (red) methods, as a function of C_Q (in steps of 0.5 MHz for 2–3 and steps of 1 MHz thereafter). Simulations were performed for a single ^{27}Al (I = 5/2) nucleus at $B_0 = 14.1$ T, $\eta_Q = 0$, $\nu_1 = 80$ kHz and MAS rates, ν_R, of (a) 12.5 kHz, (b) 40 kHz and (c) 60 kHz.

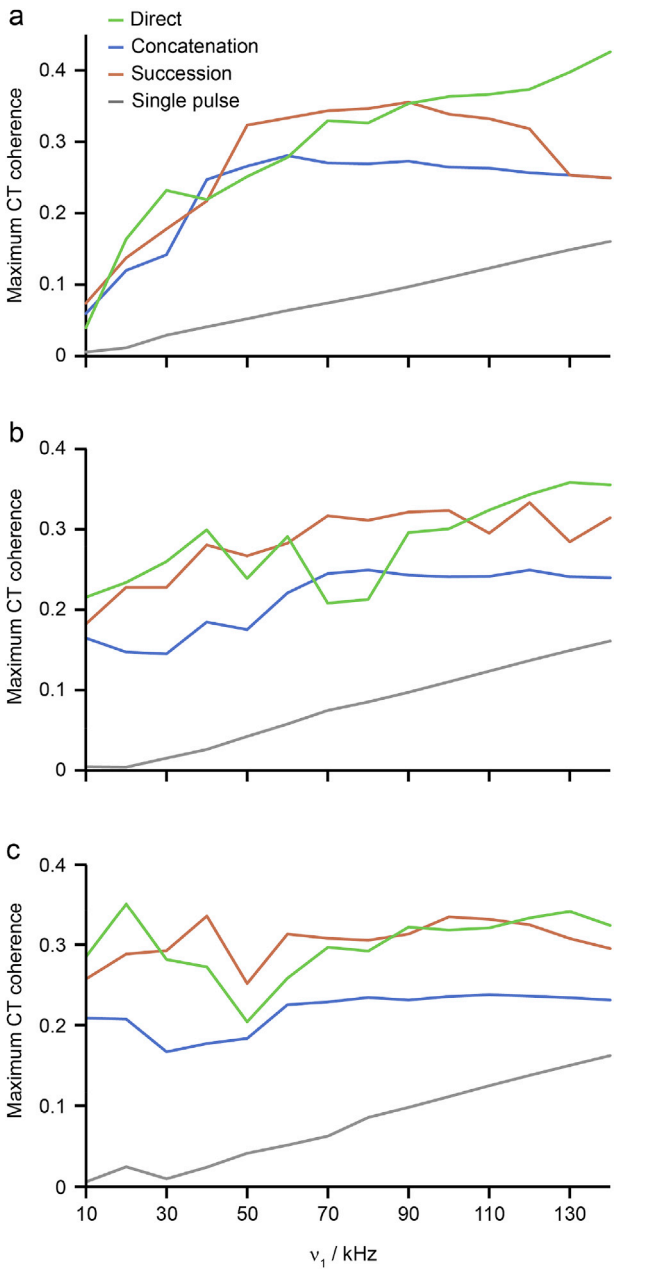

Fig. 5. Plots of the maximum CT coherence obtained from unit 5Q coherence using an optimised single pulse (grey), or FAM-N pulses generated using the direct (green), concatenation (blue) and succession (red) methods, as a function of the rf nutation rate, ν_1 (in steps of 10 kHz). Simulations were performed for a single ^{27}Al (I = 5/2) nucleus at $B_0 = 14.1$ T, $C_Q = 3.0$ MHz, $\eta_Q = 0$, and ν_R of (a) 12.5 kHz, (b) 40 kHz and (c) 60 kHz.

clear that significant enhancements (*i.e.*, I/I_0 of between 2 and 3) are once again observed (particularly at $\nu_1 = 60$ kHz) with all three methods. At the lower nutation rate the direct method has slightly lower efficiency whilst at the higher nutation rate the efficiencies of all three are very similar. It can be seen that single pulse conversion has particularly poor efficiency at low rf nutation rate and higher MAS rate. The lineshapes observed for the different approaches vary more at higher MAS rates and lower rf nutation rates, although distortions are most significant for the spectra acquired using single pulse conversion.

Table 1 shows the magnitude of the CT coherence (generated from unit 5Q coherence) obtained in simulation during the optimisation of the pulses used in the experimental measurements shown in Fig. 6. These results are in broad agreement with experiment. Although similar results are seen for all three methods, at the higher rf nutation rate, simulation predicts the direct method to be (slightly) more efficient than succession at the lower MAS, with the reverse true as the MAS rate increases. The concatenation approach is predicted to be the least efficient in each case. Experimentally, the direct method has (slightly) higher efficiency than the succession method at all MAS rates, although the gain is less as the MAS rate increases. At the lower nutation rate, simulation predicts succession to be the most efficient, and concatenation the least (for all MAS rates), in reasonably good agreement with experiment. The concatenation approach is predicted by simulation to be the least efficient under most conditions, although experimentally it is seen to improve in relative

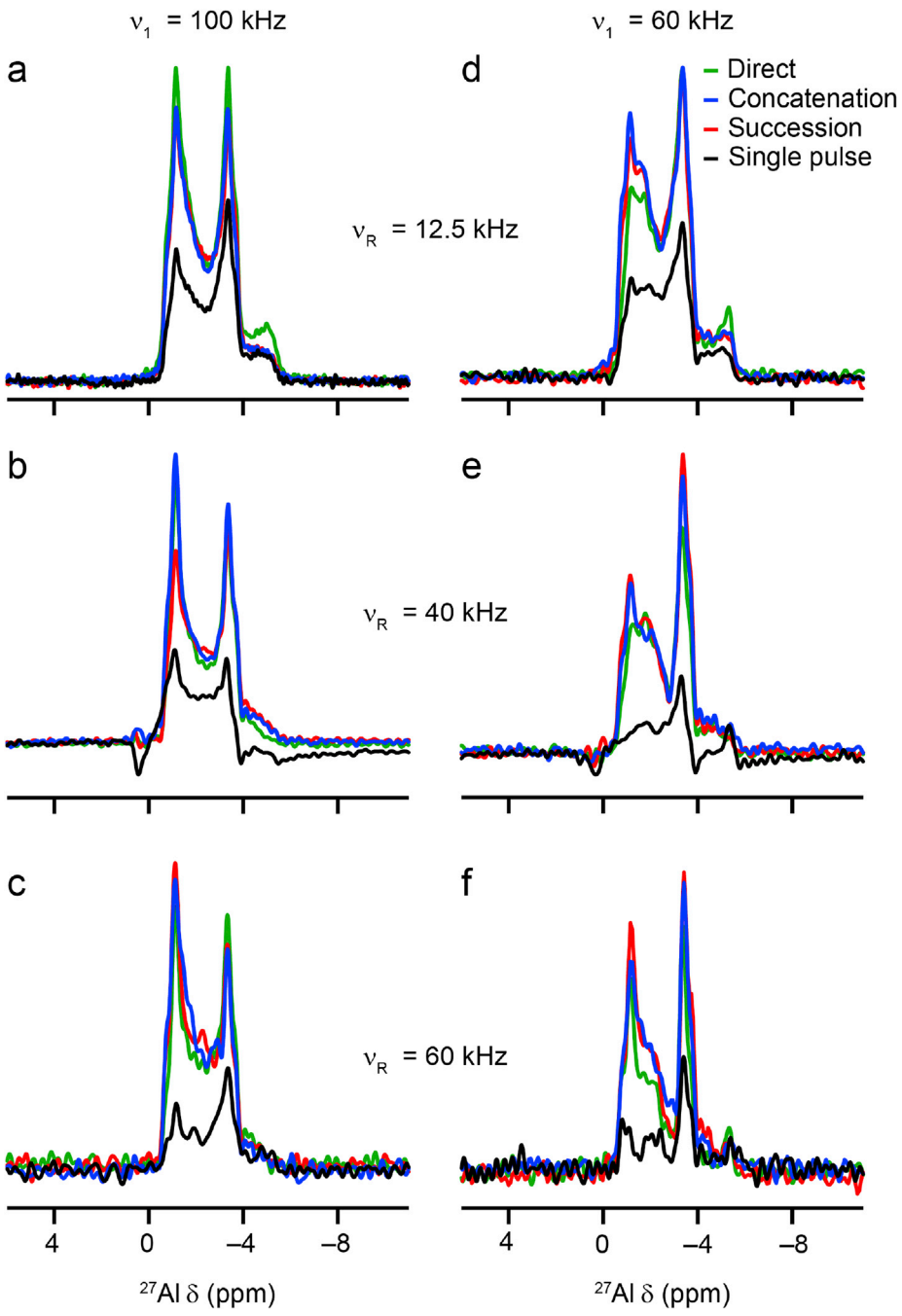

Fig. 6. ^{27}Al (14.1 T) 5Q filtered MAS NMR spectra of $Al(acac)_3$, acquired using an rf nutation rate, ν_1, of (a–c) 100 kHz and (d–f) 60 kHz at MAS rates, ν_R, of (a, d) 12.5, (b, e) 40 and (c, f) 60 kHz, using an optimised single pulse (black), or FAM-N pulses generated using the direct (green), concatenation (blue) and succession (red) methods for conversion of 5Q coherences. Spectra are the result of averaging (a) 200, (b) 2400, (c) 2000, (d) 200, (e) 2400 and (f) 3200 transients, with a recycle interval of 3 s. See Table S1.1 for further details of the FAM-N conversion pulses used.

Table 1
Amount of CT coherences generated (in simulation) from unit 5Q coherences using parameters that were employed in the experimental measurements for $Al(acac)_3$ (shown in Fig. 6).

Compound	ν_R/kHz	ν_1/kHz	FAM-N Method		
			Direct	Concatenation	Succession
$Al(acac)_3$	12.5	60	0.27	0.26	0.32
	40.0	60	0.23	0.22	0.29
	60.0	60	0.24	0.20	0.28
$Al(acac)_3$	12.5	100	0.34	0.26	0.33
	40.0	100	0.26	0.24	0.31
	60.0	100	0.28	0.23	0.32

performance at the higher MAS rates. It is worth noting, as shown in Table S1.1 in the Supporting Information, that at the higher rf nutation rates there is little difference in the total pulse duration between the concatenation and succession approaches, although the direct pulse duration is considerably shorter at higher MAS rates. Table S1.1 also shows that at the lower rf nutation rates the total duration of all three types of FAM-N pulses are much longer, and much more similar. Although the simulations assume ideal coherence selection and take no account of any effects of rf inhomogeneity and relaxation, the generally good agreement with experiment suggests that these effects (while no doubt contributing to absolute efficiencies) do not have a significant impact on the relative efficiencies of the different conversion methods.

It is clear from Fig. 6 that using FAM-N pulses for 5Q conversion is

preferred to a single pulse, and that experimentally there is often relatively little to choose between the three approaches. Corresponding results are shown in the Supporting Information for Al(lactate)$_3$ and Al(acetate)$_2$(OH), which each have a single ^{27}Al site, with higher quadrupolar coupling constants (of 5 and 8 MHz, respectively) [41]. For the lactate ($C_Q = 5$ MHz, $\nu_Q^{PAS} = 375$ kHz), the experimental efficiency of the direct approach is very poor at the lower MAS rate (poorer than the single pulse experiment – although it should be noted the latter was optimised experimentally) but increases significantly at faster spinning speeds. The efficiency of the concatenation and succession approaches is similar in all cases, giving rise to a sensitivity gains (I/I_0) between ~1.6 (at the lowest MAS rate) and ~2.5. As shown in Table S1.1 there are no significant differences in the total pulse durations between the three approaches (although all increase with an increase in the MAS rate). For Al(acetate)$_2$(OH), with higher quadrupolar coupling ($C_Q = 8$ MHz, $\nu_Q^{PAS} = 600$ kHz), poor efficiency is once again observed for the direct method at the lowest MAS rate (with little gain over single pulse conversion), although the succession and concatenation approaches give similar gains of $I/I_0 \approx 1.7$. The efficiency of the direct approach increases with MAS rate, as seen for the lactate. Maximum sensitivity gains of I/I_0 between 3.2 and 3.4 are obtained at MAS rates of 40 and 60 kHz.

The spectra in Fig. 6, and those for Al(lactate)$_3$ and Al(acetate)$_2$(OH) in the Supporting Information, contain only one distinct Al signal, enabling the exact quadrupolar parameters to be easily determined from the MAS spectrum and used in the FAM-N optimisation procedure. However, the aim of many (if not most) MQMAS experiments is to resolve signals from distinct sites that are overlapped in an MAS spectrum, and hence obtain site-specific information. In most cases, these species will have different quadrupolar parameters and, in principle, maximum enhancement should require differently optimised FAM-N pulses. This perhaps raises the more general question of whether it is worth using any such sensitivity enhancement approaches if their efficiencies depend significantly on the nature of the species present. In response to this, it is worth noting that for some MQMAS experiments (and in particular for those involving 5Q coherences) sensitivity can truly be limiting, and enhancements are vital to make experiments possible either at all, or on a sensible timescale. Furthermore, the lack of any requirement for experimental optimisation for FAM-N means that this does not affect the time required for experimental acquisition, and so any enhancement comes "for free" and, unless a decrease in sensitivity relative to a single pulse is predicted, it should be worth applying a FAM-N pulse, even if this is not optimised for any/all of the species present. For 3QMAS experiments, optimised FAM-N pulses were shown to be robust relative variation in C_Q and ν_1, with good enhancements achieved over reasonable ranges of these parameters [36,37], and an improvement over single pulse conversion observed in all but the most extreme cases.

Fig. 7 plots the ^{27}Al CT coherence generated (in simulation) from unit 5Q coherences using either a single pulse or one of the three different FAM-N pulses, as a function of C_Q. In this case (and unlike the plots in Fig. 4), the FAM-N pulses were optimised for one value of C_Q (*i.e.*, 3 and 5 MHz in a and b, respectively), and these same pulses were then employed for varying C_Q values. (Other simulation parameters are $B_0 = 14.1$ T, $\nu_R = 12.5$ kHz and $\nu_1 = 100$ kHz). Good enhancements over a single pulse are seen for all FAM-N methods at the C_Q values at which the pulses were optimised, but significant enhancements are also observed across the range of C_Q values tested. The FAM-N pulses generated using succession and concatenation approaches behave similarly as the magnitude of C_Q changes, but the pulses generated for direct 5Q → CT transfer behave in a similar manner to the single pulse conversion (*i.e.*, with a more significant decrease in efficiency as C_Q increases). It should be noted that although the direct method has poorer efficiency at C_Q values higher than those for which they were generated, the efficiency at lower C_Q is higher and does not drop below that for a single pulse at any point. For concatenation and succession pulses, enhancements are more similar across the range of C_Q values, but do approach that of single pulse conversion at very low C_Q. However, Fig. 7 suggests that any of the FAM-N pulses should be useful for improving the efficiency of 5Q conversion on multisite samples, leading to significant enhancements for species with all but the most extreme C_Q values. To mitigate any possible signal loss it seems clear that it would be best to generate the FAM-N pulses using C_Q values that are in reasonable agreement with those for the majority of species present or, where this is not possible, for a value close to the average of those seen experimentally.

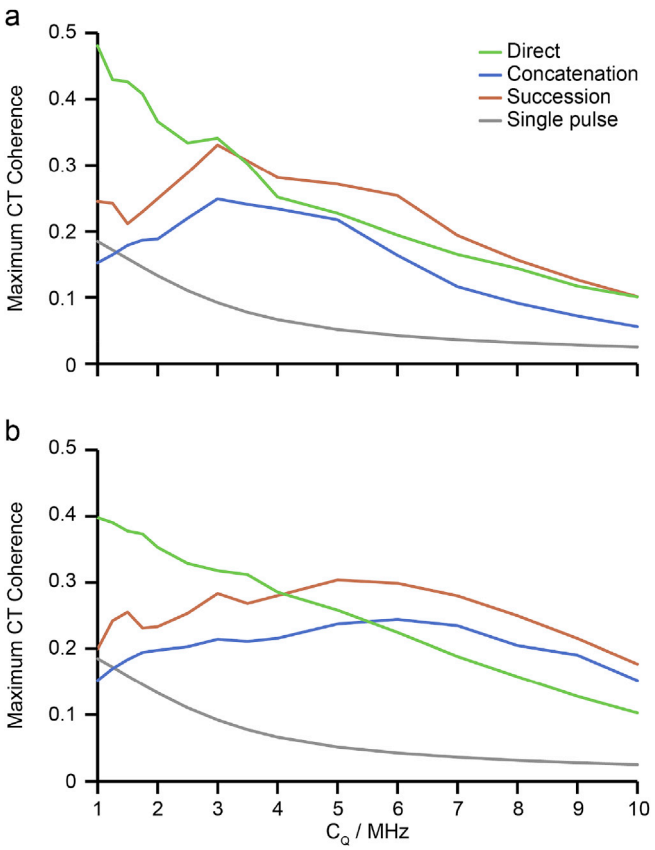

Fig. 7. Plot of the amount of ^{27}Al CT coherence obtained from unit 5Q coherence using an optimised single pulse (grey), or FAM-N pulses generated using the direct (green), concatenation (blue) and succession (red) methods as a function of C_Q (in steps of 0.25 MHz from 1 to 2 and steps of 0.5 MHz thereafter). The FAM-N pulses were generated using $B_0 = 14.1$ T, C_Q = (a) 3.0 MHz and (b) 5.0 MHz, $\eta_Q = 0.15$, $\nu_1 = 100$ kHz and $\nu_R = 12.5$ kHz and were not reoptimised for different C_Q values.

Fig. 8 plots the experimental signal intensity in ^{27}Al 5Q filtered MAS NMR spectra of Al(acac)$_3$, as a function of the rf nutation rate, for FAM-N pulses optimised for a fixed value of ν_1 (60 kHz) but then applied at different values, for MAS rates of (a) 12.5 and (b) 40 kHz. The signal intensity is plotted relative to the intensity obtained for a single pulse conversion at an rf nutation rate of 60 kHz. Fig. 8a shows that at the lower MAS rate the performance of all three approaches is very similar, with good efficiency over most of this range, decreasing slightly at higher ν_1. Larger differences in overall efficiency are seen at the higher MAS rate (Fig. 8b), with the succession FAM-N pulse slightly more efficient over the entire range. However, similar behaviour is seen for the three FAM-N approaches as ν_1 varies.

As seen in previous work for 3Q conversion [36,37], FAM-N pulses generated for 5Q conversion typically give good sensitivity enhancements over a single pulse, and are robust to variation of the experimental parameters. When combined with the lack of any time-consuming experimental optimisation, these properties make FAM-N particularly attractive for use on more challenging samples, *i.e.*, those with very poor sensitivity. Such limited sensitivity may result from low γ (affecting both the overall sensitivity, the rf nutation rates that can be achieved and the

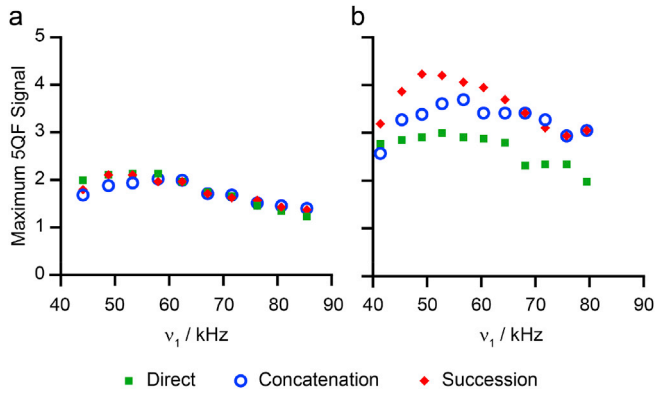

Fig. 8. Plot showing the (integrated) signal intensity in ^{27}Al (14.1 T) 5Q filtered MAS NMR spectra of Al(acac)$_3$ at (a) $\nu_R = 12.5$ kHz and (b) $\nu_R = 40$ kHz using FAM-N pulses generated using the direct (green squares), concatenation (blue circles) and succession (red diamonds) methods for conversion of 5Q coherences, as a function of ν_1. The signal intensity is plotted relative to that obtained for a single pulse conversion at the rf nutation rate of 60 kHz. FAM-N pulses were optimised for $B_0 = 14.1$ T, $C_Q = 3$ MHz, $\eta_Q = 0.15$, $\nu_1 = 60$ kHz and ν_R = (a) 12.5 kHz and (b) 40 kHz but applied at different ν_1. Data are the result of averaging (a) 40 and (b) 80 transients, with a recycle interval of 3 s. See Table S1.1 for further details of the FAM-N conversion pulses used.

magnitude of the quadrupolar broadening observed), low natural or chemical abundance of an isotope, limited sample volume or, alternatively, from a combination of these. It is in these cases where FAM-N will be invaluable for achieving high-resolution spectra either on a reasonable timescale or, indeed, at all. One potential application of this work is the ^{17}O NMR study of silicate minerals [42]. These materials play a vital role in the Earth's interior, and in determining the physical and chemical properties of the planet. ^{17}O (I = 5/2) NMR spectroscopy has been shown to be a crucial tool in understanding local structure and, in particular, disorder in these materials, but the low natural abundance of ^{17}O (~0.037%) prevents routine study. Although isotopic enrichment is possible [43], the high cost of enriched reagents requires cost- and atom-efficient synthetic approaches and can limit the enrichment level that can be achieved at reasonable cost. Furthermore, the high pressures required for synthesis can produce relatively small sample volumes, again limiting sensitivity. In most cases, there are several distinct O sites present and high-resolution approaches are required to obtain site-specific information. While 3QMAS and 5QMAS have been employed to study anhydrous and hydrous inner Earth minerals (with the 5QMAS spectra showing better resolution) [27,28,44,45], in more challenging cases STMAS has been employed owing to the increased sensitivity [46,47]. As the complexity of the system under study increases, there will be a need for improved resolution and the use of 5QMAS, rather than 3QMAS, experiments.

Fig. 9 shows ^{17}O 5Q filtered NMR spectra of forsterite (35% enriched in ^{17}O), the α polymorph of Mg_2SiO_4, and the major component of the Earth's upper mantle down to depths of 400 km. Although forsterite can be synthesised at atmospheric pressure (and therefore on a reasonable scale), this is a good model system for evaluating the efficiency of FAM-N pulses, as the corresponding experiment with single pulse conversion is also possible. Fig. 9 shows that at the conditions used ($B_0 = 14.1$ T, $\nu_1 = 65$ kHz and $\nu_R = 12.5$ kHz), all three FAM-N methods give a significant enhancement over a single pulse conversion (despite the latter being experimentally optimised). The succession approach appears most efficient (giving a signal gain of $I/I_0 \approx 2.3$), although good enhancements are also obtained with the direct and concatenation approaches. Although three ^{17}O sites are present in this material, all three have similar C_Q values (of 2.4–2.8 MHz, ν_Q^{PAS} of 180–210 kHz) [27], and this is reflected in the fairly uniform enhancements over the entire lineshape.

Fig. 10 shows ^{45}Sc 5Q filtered MAS NMR spectra of scandium oxide (Sc_2O_3), acquired at 20.0 T at two different MAS rates. This material has

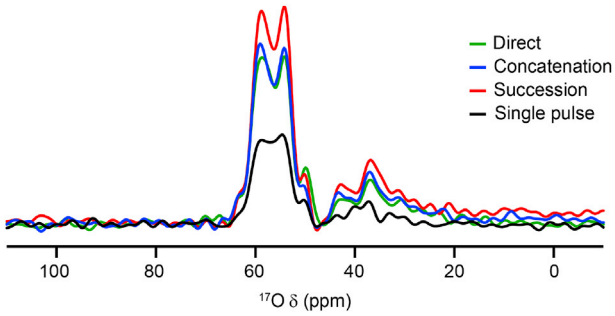

Fig. 9. ^{17}O (14.1 T) 5Q filtered MAS NMR spectra of forsterite (α-Mg_2SiO_4), acquired with $\nu_1 = 65$ kHz and $\nu_R = 12.5$ kHz, using an optimised single pulse (black), or FAM-N pulses generated using the direct (green), concatenation (blue) and succession (red) methods for conversion of 5Q coherences. Spectra are the result of averaging 13200 transients, with a recycle interval of 6 s. See Table S1.1 for further details of the FAM-N conversion pulses used.

two distinct ^{45}Sc sites, both with large quadrupolar couplings (23.4 MHz for Sc1 and 15.3 MHz for Sc2, giving $\nu_Q^{PAS} = 821$ and 546 kHz, respectively) [48], necessitating the use of high field and fast MAS. The different relative intensities of the two sites (1:3) and the increased broadening associated with Sc1 means it is more challenging to observe this site, particularly without the use of a spin echo sequence. The 5Q filtered signal in Fig. 10 therefore results primarily from Sc2, and the FAM-N pulses were optimised for parameters corresponding to this site (*i.e.*, $C_Q = 15.3$ MHz and $\eta_Q = 0.63$). Good sensitivity gains are apparent at both MAS rates, demonstrating the applicability of this approach to nuclei high higher spin quantum number. At the lower MAS rate (Fig. 10a), the direct method once again has poor sensitivity (with little improvement over single pulse conversion), while the concatentation and succession approaches give gains of $I/I_0 \approx 1.4$ (and a time saving of a factor of ~2). The gains are higher at the faster MAS rate, with all three approaches giving an increase of $I/I_0 \approx 1.7$ (and a saving of ~2.9 in time).

4. Conclusions

The increased shift dispersion that 5QMAS experiments can offer over the more commonly used 3QMAS methods makes their application attractive, or in fact required, when the highest resolution is needed. However, the significant decrease in sensitivity that accompanies the filtration through higher-order MQ coherences poses a significant challenge to their implementation and wider use. We have demonstrated that FAM-N pulses can be used to improve the efficiency of MQ conversion, providing an approach that is easy to implement and which requires no direct experimental optimisation. Significant enhancements (typically of $I/I_0 = 1.5$–3) are obtained over a single pulse conversion for all three FAM-N methods considered, for all but the most extreme experimental conditions. While the exact efficiency of each approach varies with the rf nutation rate, MAS rate and quadrupolar parameters, broadly similar results are obtained for all three types of pulses in most cases, although the experimental efficiency of the direct approach is often poorer at lower MAS rates for sites with high C_Q. This may well be due to the effects of rf inhomogeneity in the larger rotor, or perhaps due to relaxation (which is not included in the simulation). However, further experimental and computational investigation would be required to understand the origin of this observation.

In general, good agreement was obtained between simulation and experiment, confirming that FAM-N pulses can be applied as obtained from the high-throughput optimisation, avoiding time consuming experimental optimisation. The best signal enhancements are obtained with prior knowledge of C_Q values (which can often be estimated from MAS spectra or predicted using DFT calculations) and the experimental parameters (*i.e.*, ν_1 and ν_R). However, in most cases, good enhancements can be obtained for all three FAM-N methods even when they are applied

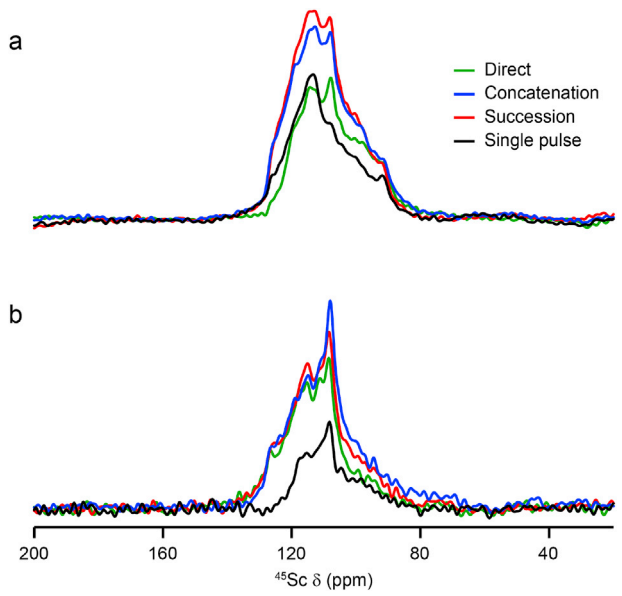

Fig. 10. ^{45}Sc (20.0 T) 5Q filtered MAS NMR spectra of scandium oxide (Sc_2O_3), acquired with $\nu_1 = 80$ kHz at MAS rates, ν_R, of (a) 20 and (c) 60 kHz, using an optimised single pulse (black), or FAM-N pulses generated using the direct (green), concatenation (blue) and succession (red) methods for conversion of 5Q coherences. Spectra are the result of averaging (a) 40,000 and (b) 120,000 transients, with a recycle interval of 0.25 s. See Table S1.1 for further details of the FAM-N conversion pulses used.

under conditions that are different to those for which they were optimised. The robustness of the approaches varies little. However, for FAM-N pulses applied to systems with a different C_Q to that for which they were generated (a situation that is inherent in MQMAS experiments on most multi-site samples), the succession and concatenation methods show the least variation in efficiency across a wider range of C_Q, but potentially larger enhancements are available under some conditions using the direct approach. Given the simplicity of this latter approach, it may well be the method of choice at higher MAS rates for application to challenging systems, *i.e.*, those with low sample volumes, low-γ nuclei or nuclei with low natural abundance. However, for experiments at lower MAS rates the alternative approaches are probably preferred, as discussed above.

We believe that, in addition to their use for 3QMAS experiments, FAM-N pulses offer a simple, robust and efficient approach for improving the conversion of 5Q coherences within the context of the MQMAS experiment. We have demonstrated their use for nuclei with I = 5/2 and 7/2, and their application, particularly at faster MAS rates where lower sample volumes are available, and at the lower rf nutation rates available for low-γ nuclei, should ease the application of MQMAS for more challenging, more important and more interesting systems.

Acknowledgements

We would like to thank the ERC (EU FP7 Consolidator Grant 614290 "EXONMR") and EPSRC (award of a studentship to HC through EP/K503162/1). SEA would also like to thank the Royal Society and Wolfson Foundation for a merit award. The UK 850 MHz solid-state NMR Facility used in this research was funded by EPSRC and BBSRC (contract reference PR140003), as well as the University of Warwick including via part funding through Birmingham Science City Advanced Materials Projects 1 and 2 supported by Advantage West Midlands (AWM) and the European Regional Development Fund (ERDF). Collaborative assistance from the 850 MHz Facility Manager (Dinu Iuga, University of Warwick) is acknowledged. The research data supporting this publication can be accessed at DOI: 10.17630/04b0c37f-b803-4dd7-b13a-2004b0b5c482.[49].

Appendix A. Supplementary data

Supplementary data to this article can be found online at https://doi.org/10.1016/j.ssnmr.2019.03.002.

References

[1] E.R. Andrew, Magic Angle Spinning. eMagRes, Wiley, New York, 2007, https://doi.org/10.1002/9780470034590.emrstm0283.
[2] D.C. Apperley, R.K. Harris, P. Hodgkinson, Solid State NMR Basic Principles and Practice, Momentum Press, New York, 2012, https://doi.org/10.5643/9781606503522.
[3] S.E. Ashbrook, D.M. Dawson, J.M. Griffin, Solid-state NMR spectroscopy, in: D.W. Bruce (Ed.), Local Structural Characterisation, John Wiley & Sons Ltd, Chichester, 2014, pp. 1–88.
[4] S.E. Ashbrook, S. Sneddon, New methods and applications in solid-state NMR spectroscopy of quadrupolar nuclei, J. Am. Chem. Soc. 136 (2014) 15440–15456, https://doi.org/10.1021/ja504734p.
[5] A. Samoson, E. Lippmaa, A. Pines, High resolution solid-state NMR, Mol. Phys. 65 (1988) 1013–1018, https://doi.org/10.1080/00268978800101571.
[6] A. Llor, J. Virlet, Towards high-resolution NMR of more nuclei in solids – sample spinning with time-dependent spinner Axis Angle, J. Chem. Phys. Lett. 152 (1988) 248–253, https://doi.org/10.1016/0009-2614(88)87362-7.
[7] L. Frydman, J.S. Harwood, Isotropic spectra of half-integer quadrupolar spins from bidimensional magic-angle-spinning NMR, J. Am. Chem. Soc. 117 (1995) 5367–5368, https://doi.org/10.1021/ja00124a023.
[8] A. Goldburt, P.K. Madhu, Multiple-quantum magic-angle spinning: high-resolution solid-state NMR of half-integer spin quadrupolar nuclei, Annu. Rep. NMR Spectrosc. 54 (2004) 81–153, https://doi.org/10.1016/s0066-4103(04)54003-6.
[9] J. Rocha, C.M. Morais, C. Fernandez, Progress in multiple-quantum magic-angle spinning NMR spectroscopy, Top. Curr. Chem. 246 (2005) 141–194, https://doi.org/10.1007/b98650.
[10] J.P. Amoureux, C. Fernandez, L. Frydman, Optimized multiple-quantum magic-angle spinning NMR experiments on half-integer quadrupoles, Chem. Phys. Lett. 259 (1996) 347–355, https://doi.org/10.1016/0009-2614(96)00809-3.
[11] J.P. Amoureux, M. Pruski, D.P. Lang, C. Fernandez, The effect of RF power and spinning speed on MQMAS NMR, J. Magn. Reson. 131 (1998) 170–175, https://doi.org/10.1006/jmre.1997.1275.
[12] Z. Gan, Isotropic NMR spectra of half-integer quadrupolar nuclei using satellite transitions and magic-angle spinning, J. Am. Chem. Soc. 122 (2000) 3242–3243, https://doi.org/10.1021/ja9939791.
[13] S.E. Ashbrook, S. Wimperis, High-resolution NMR of quadrupolar nuclei in solids: the satellite-transition magic angle spinning (STMAS) experiment, Prog. Nucl. Magn. Reson. Spectrosc. 45 (2004) 53–108, https://doi.org/10.1016/j.pnmrs.2004.04.002.
[14] T.J. Ball, S. Wimperis, Use of SPAM and FAM pulses in high-resolution MAS NMR spectroscopy of quadrupolar nuclei, J. Magn. Reson. 187 (2007) 343–351, https://doi.org/10.1016/j.jmr.2007.05.020.
[15] A.P.M. Kentgens, R. Verhagen, Advantages of double frequency sweeps in static, MAS and MQMAS NMR of spin I = 3/2 nuclei, Chem. Phys. Lett. 300 (1999) 435–443, https://doi.org/10.1016/s0009-2614(98)01402-x.
[16] P.K. Madhu, A. Goldbourt, L. Frydman, S. Vega, Sensitivity engancement of the MQMAS NMR experiment by fast amplitude modulation of the pulses, Chem. Phys. Lett. 307 (1999) 41–47, https://doi.org/10.1016/s0009-2614(99)00446-7.
[17] P.K. Madhu, A. Goldbourt, L. Frydman, S. Vega, Fast radio-frequency amplitude modulation in multiple-quantum magic-angle-spinning nuclear magnetic resonance: theory and experiments, J. Chem. Phys. 112 (2000) 2377–2391, https://doi.org/10.1063/1.480804.
[18] Z. Gan, H.-T. Kwak, Enhancing MQMAS sensitivity using signals from multiple coherence transfer pathways, J. Magn. Reson. 168 (2004) 346–351, https://doi.org/10.1016/j.jmr.2004.03.021.
[19] J.P. Amoureux, L. Delevoye, S. Steuernagel, Z. Gan, S. Ganapathy, L. Montagne, Increasing the sensitivity of 2D high-resolution NMR methods applied to quadrupolar nuclei, J. Magn. Reson. 172 (2005) 268–278, https://doi.org/10.1016/j.jmr.2004.11.001.
[20] R. Siegel, T.T. Nakashima, R.E. Wasylishen, Sensitivity enhancement of MQMAS NMR spectra of spin 3/2 nuclei using hyperbolic secant pulses, Chem. Phys. Lett. 403 (2005) 353–358, https://doi.org/10.1016/j.cplett.2005.01.023.
[21] J.P. Amoureux, C. Fernandez, Triple, quintuple and higher order multiple quantum MAS NMR of quadrupolar nuclei, Solid State Nucl. Magn. Reson. 10 (1998) 211–223, https://doi.org/10.1016/s0926-2040(97)00027-1.
[22] K.J. Pike, R.P. Malde, S.E. Ashbrook, J. McManus, S. Wimperis, Multiple-quantum MAS NMR of quadrupolar nuclei. Do five-, seven- and nine-quantum experiments yield higher resolution than the three-quantum experiment? Solid State Nucl. Magn. Reson. 16 (2000) 203–215, https://doi.org/10.1016/s0926-2040(00)00081-3.
[23] S.P. Brown, S.E. Ashbrook, S. Wimperis, ^{27}Al multiple-quantum magic angle spinning NMR study of the thermal transformation between the microporous aluminum methylphosphonates AlMePO-β and AlMePO-α, J. Phys. Chem. B 103 (1999) 812–817, https://doi.org/10.1021/jp9824858.
[24] C. Fernandez, J.P. Amoureux, 2D multiquantum MAS-NMR spectroscopy of ^{27}Al in aluminophosphate molecular sieves, Chem. Phys. Lett. 242 (1995) 449–454, https://doi.org/10.1016/0009-2614(95)00768-y.
[25] J. Rocha, J.P. Lourenco, M.F. Ribeiro, C. Fernandez, J.P. Amourex, Multiple-quantum ^{27}Al MAS NMR spectroscopy of microporous AlPO-40 and

SAPO-40, Zeolites 19 (1997) 156–160, https://doi.org/10.1016/s0144-2449(97)00062-6.
[26] P.S. Neuhoff, P. Zhao, J.F. Stebbins, Effect of extraframework species on ^{17}O NMR chemical shifts in zeolite A, Microporous Mesoporous Mater. 55 (2002) 239–251, https://doi.org/10.1016/S1387-1811(02)00413-4.
[27] S.E. Ashbrook, A.J. Berry, S. Wimperis, Three- and five-quantum ^{17}O MAS NMR of forsterite Mg_2SiO_4, Am. Mineral. 84 (1999) 1191–1194, https://doi.org/10.2138/am-1999-7-824.
[28] S.E. Ashbrook, A.J. Berry, S. Wimperis, ^{17}O multiple-quantum MAS NMR study of high-pressure hydrous magnesium silicates, J. Am. Chem. Soc. 123 (2001) 6360–6366, https://doi.org/10.1021/ja004290v.
[29] S.R. Jansen, H.T. Hintzen, R. Metselaar, J.W. de Haan, L.J.M. van de Ven, A.P.M. Kengens, G.H. Nachtegaal, Multiple quantum ^{27}Al magic-angle-spinning nuclear magnetic resonance spectroscopic study of $SrAl_{12}O_{19}$: identification of a ^{27}Al resonance from a well-defined AlO_5 site, J. Phys. Chem. B 102 (1998) 5969–5976, https://doi.org/10.1021/jp981224v.
[30] S.E. Ashbrook, S. Wimperis, Multiple-quantum cross-polarization and two-dimensional MQMAS NMR of quadrupolar nuclei, J. Magn. Reson. 147 (2000) 238–249, https://doi.org/10.1006/jmre.2000.2174.
[31] C.V. Chandran, J. Cuny, R. Gautier, L. Le Polles, C.J. Pickard, T. Brauniger, Improving sensitivity and resolution of MQMAS spectra: a ^{45}Sc-NMR case study of scandium sulphate pentahydrate, J. Magn. Reson. 203 (2010) 226–235, https://doi.org/10.1016/j.jmr.2009.12.021.
[32] D. Iuga, H. Schafer, R. Verhagen, A.P.M. Kentgens, Population and coherence transfer induced by double frequency sweeps in half-integer quadrupolar spin systems, J. Magn. Reson. 147 (2000) 192–209, https://doi.org/10.1006/jmre.2000.2192.
[33] T. Vosegaard, D. Massiot, P.J. Garndinetti, Sensitivity enhancements in MQ-MAS NMR of spin-5/2 nuclei using modulated Rf mixing pulses, Chem. Phys. Lett. 326 (2000) 454–460, https://doi.org/10.1016/s0009-2614(00)00779-x.
[34] T. Bräuniger, K.J. Pike, R.K. Harris, P.K. Madhu, Efficient 5QMAS NMR of spin-5/2 nuclei: use of fast amplitude-modulated radio-frequency pulses and cogwheel phase cycling, J. Magn. Reson. 163 (2003) 64–72, https://doi.org/10.1016/S1090-7807(03)00124-1.
[35] A. Goldbourt, S. Vega, Signal enhancement in 5QMAS spectra of spin-5/2 quadrupolar nuclei, J. Magn. Reson. 154 (2002) 280–286, https://doi.org/10.1006/jmre.2001.2475.
[36] H. Colaux, D.M. Dawson, S.E. Ashbrook, Efficient amplitude-modulated pulses for triple-to single-quantum coherence conversion in MQMAS NMR, J. Phys. Chem. A 118 (2014) 6018–6025, https://doi.org/10.1021/jp505752c.
[37] H. Colaux, D.M. Dawson, S.E. Ashbrook, Investigating FAM-N pulses for signal enhancement in MQMAS NMR of quadrupolar nuclei, Solid State Nucl. Magn. Reson. 84 (2017) 89–102, https://doi.org/10.1016/j.ssnmr.2017.01.001.
[38] C.M. Morais, M. Lopes, C. Fernandez, J. Rocha, Assessing the potential of fast amplitude modulation pulses for improving triple-quantum magic angle spinning NMR spectra of half-integer quadrupolar nuclei, Magn. Reson. Chem. 41 (2003) 679–688, https://doi.org/10.1002/mrc.1238.
[39] M. Bak, J. Rasmussen, N. Nielsen, SIMPSON: a general simulation program for solid-state NMR spectroscopy, J. Magn. Reson. 147 (2000) 296–330, https://doi.org/10.1006/jmre.2000.2179.
[40] P.J. Barrie, Distorted powder lineshapes in ^{27}Al CP MAS NMR spectroscopy of solids, Chem. Phys. Lett. 208 (1993) 486–490, https://doi.org/10.1016/0009-2614(93)87177-5.
[41] L. van Wullen, M. Kalwei, ^{13}C–^{27}Al TRAPDOR and REDOR experiments for the detection of ^{13}C–^{27}Al dipolar interactions in solids, J. Magn. Reson. 139 (1999) 250–257, https://doi.org/10.1006/jmre.1999.1765.
[42] J.M. Griffin, S.E. Ashbrook, Solid-state NMR of high-pressure silicates in the Earth's mantle, Annu. Rep. NMR Spectrosc. 79 (2013) 241–332, https://doi.org/10.1016/b978-0-12-408098-0.00005-7.
[43] S.E. Ashbrook, M.E. Smith, Solid state ^{17}O NMR - an introduction to the background principles and applications to inorganic materials, Chem. Soc. Rev. 35 (2006) 717–735, https://doi.org/10.1039/b514051j.
[44] S.E. Ashbrook, A.J. Berry, D.J. Frost, A. Gregorovic, C.J. Pickard, J.E. Readman, S. Wimperis, ^{17}O and ^{29}Si NMR parameters of $MgSiO_3$ phases from high-resolution solid-state NMR spectroscopy and first-principles calculations, J. Am. Chem. Soc. 129 (2007) 13213–23224, https://doi.org/10.1021/ja074428a.
[45] J.M. Griffin, S. Wimperis, A.J. Berry, C.J. Pickard, S.E. Ashbrook, Solid-state ^{17}O NMR spectroscopy of hydrous magnesium silicates: evidence for proton dynamics, J. Phys. Chem. C 113 (2009) 465–471, https://doi.org/10.1021/jp808651x.
[46] S.E. Ashbrook, A.J. Berry, W.O. Hibberson, S. Steuernagel, S. Wimperis, High-resolution ^{17}O NMR spectroscopy of wadsleyite (β-Mg_2SiO_4), J. Am. Chem. Soc. 125 (2003) 11824–11825, https://doi.org/10.1021/ja036777k.
[47] J.M. Griffin, A.J. Berry, D.J. Frost, S. Wimperis, S.E. Ashbrook, Water in the earth's mantle: a solid-state NMR study of hydrous wadsleyite, Chem. Sci. 4 (2013) 1523–1538, https://doi.org/10.1039/c3sc21892a.
[48] N. Kim, C.-H. Hsieh, J.F. Stebbins, Scandium coordination in solid oxides and stabilized zirconia: ^{45}Sc NMR, Chem. Mater. 18 (2006) 3855–3859, https://doi.org/10.1021/cm060590l.
[49] N. Kanwal, H. Colaux, D.M. Dawson, Y. Nishiyama, S.E. Ashbrook, Sensitivity Improvement in 5QMAS NMR Experiments Using FAM-N Pulses (Dataset), University of St Andrews Research Portal, 2019. https://doi.org/10.17630/04b0c37f-b803-4dd7-b13a-2004b0b5c482.